

Synthesis and characterization of cellulose nanocrystals as reinforcing agent in solely palm based polyurethane foam

Athanasia Amanda Septevani, Pratheep K. Annamalai, and Darren J. Martin

Citation: [AIP Conference Proceedings](#) **1904**, 020042 (2017); doi: 10.1063/1.5011899

View online: <https://doi.org/10.1063/1.5011899>

View Table of Contents: <http://aip.scitation.org/toc/apc/1904/1>

Published by the [American Institute of Physics](#)

Articles you may be interested in

[Plasticization of poly\(lactic acid\) using different molecular weight of Poly\(ethylene glycol\)](#)

[AIP Conference Proceedings](#) **1904**, 020038 (2017); 10.1063/1.5011895

[The effect of cellulose nanocrystal \(CNC\) from rattan biomass as filler and citric acid as co-plasticizer on tensile properties of sago starch biocomposite](#)

[AIP Conference Proceedings](#) **1904**, 020043 (2017); 10.1063/1.5011900

[Effect of reaction time and polyethylene glycol monooleate-isocyanate composition on the properties of polyurethane-polysiloxane modified epoxy](#)

[AIP Conference Proceedings](#) **1904**, 020046 (2017); 10.1063/1.5011903

[Preparation of nanobiochar as magnetic solid acid catalyst by pyrolysis-carbonization from oil palm empty fruit bunches](#)

[AIP Conference Proceedings](#) **1904**, 020018 (2017); 10.1063/1.5011875

[The influenced of reaction time on the degradation of palm oil empty fruit bunch \(EFB\) in hydrothermal carbonization](#)

[AIP Conference Proceedings](#) **1904**, 020040 (2017); 10.1063/1.5011897

[Dispersion polymerization of L-lactide utilizing ionic liquids as reaction medium](#)

[AIP Conference Proceedings](#) **1904**, 020037 (2017); 10.1063/1.5011894

Synthesis and characterization of cellulose nanocrystals as reinforcing agent in solely palm based polyurethane foam

Athanasia Amanda Septevani^{1a)}, Pratheep K Annamalai², and Darren J Martin²

¹*Indonesian Institute of Sciences, Research Center for Chemistry, Serpong –Tangerang Selatan 15314, Indonesia*

²*Australian Institute for Bioengineering and Nanotechnology, The University of Queensland, Australia*

^{a)}Corresponding author: atha001@lipi.go.id

Abstract. The increasing awareness of the environment and the economy of petroleum resources has driven the development of alternative processes and raw materials based on sustainable and renewable biomaterials with excellent properties. This study is aimed to use biologically renewable cellulose nanocrystals (CNC) as reinforcing agent to enhance the properties of polyurethane foams (PUF) based on solely palm-polyol. Rod-like shape cellulose nanocrystals (CNC) was successfully isolated from cotton based resources via strong acid hydrolysis with the average width, length and aspect ratio about 14.7 ± 4.9 nm, 167.7 ± 23.2 nm and 11.4, respectively. The crystallinity of CNC was confirmed by using X-ray diffraction (XRD) and differential scanning calorimetry (DSC) and was found at 82.8% and 83.8%, respectively. This obtained cellulose nanocrystals (CNC) at a loading of 0.4 wt. % was then incorporated via solvent-free sonication method in the model of palm based polyurethane foam. The preliminary results showed that the effect of CNC on the mechanical properties afforded a significant improvement on the compressive strength and modulus without affecting much their tensile strength. The results on thermal stability and thermal transitions were found unchanged whereas the storage modulus revealed substantial improvement with the presence of CNC with almost two fold from 0.7 MPa to 1.3 MPa (~86 %).

INTRODUCTION

Cellulose, a carbohydrate with linear chain of glucose molecule, is the most abundant polymers in nature. It can be found not only in plant sources such as wood and plant (cotton, ramie, hemp, straw, wheat) but also in non-plant sources such as tunicate (family of sea animals), algae, and bacteria.^{1,2} Recently, the use of nanocellulose as reinforcing agent in various polymer matrices have gained growing interest as a new class of cellulose based “building block” due to chemically active hydroxyl groups on the surface, low density and also in addition to their abundance. In particular, rod like cellulose nanocrystals (CNC) exhibits unprecedented mechanical properties with low density; specifically the tensile strength and elastic modulus are higher than manmade materials such as cast iron and even Kevlar[®].¹ The remarkable mechanical properties (Young’s Modulus of 220 GPa and tensile strength of 7.7 GPa) are due to inter-intramolecular hydrogen bonding of hydroxyl groups on the CNC polymer.^{3,4}

Polyurethane is one of the most versatile polymers because of its wide range products (in the form of foams, coatings, and thermoplastics) and applications. Owing to their versatility and vast array of monomer variables, the range of properties for many engineering applications can be achieved. Among polyurethane products, the market segment for PUF is the largest, particularly for flexible PUF. However, with increasing awareness of the environment and the economy of petroleum resources, it has become important to look for alternative processes and raw materials for achieving good performance PUF from the renewable resources.

In recent years, considerable studies of bio-polyols have been successfully derived from both palm oil and palm kernel oil⁵⁻⁷ for synthesizing PUF. In fact, palm based polyol has been commercially produced for a range of polyurethane product. However, synthesizing flexible PUF from solely palm based polyol is still challenging such as obtaining an adequate dimensional stability and mechanical properties of PUF. Hence in this study, CNC is incorporated into solely palm oil based PUF with the aim to enhance the mechanical properties providing the

excellent mechanical properties and active chemical surface of CNC make them as the most promising candidate of physical and chemical reinforcing fillers. In this study CNC was synthesized from via acid hydrolysis from the cotton filter papers. The isolation of nanocellulose from cotton is preferred, because the higher cellulose content enables a higher yield and reduces the need for purification.² The structure-property relationship of the CNC nanocomposite PUF compared to neat PUF is also thoroughly investigated and discussed in this paper. Since, the polyol and nanoparticles are biorenewable, investigating foams thereof can be alternative natural resources for the sustainable replacement of the petroleum feedstocks and polymers.

MATERIALS AND METHODS

Materials

Cotton filter paper from Advantec was used to produce cellulose nanocrystals via a typical acid hydrolysis protocol using sulfuric acid 98% purchased from Merck. Maskimiol PKF 3000®; a palm kernel oil based polyester polyol (PKObP), was received from Maskimi Polyol SDN.BHD in Malaysia with average molecular weight 3000 and hydroxyl number 58-65 mg KOH/g. Aptane™ B900, a polymeric methylene diphenyl diisocyanates (pMDI) was received from Ariel Industries Pty. Ltd, Victoria, Australia. Silicone surfactant (Tegostab B 8905) was provided by Evonik Industries. Dibutyltin dilaurate (DBTL, tin catalyst) and N,N dimethylbenzylamine (amine catalyst) was purchased from Sigma Aldrich. All chemicals were used as received.

Methods

CNC and Foam Preparation

CNC was obtained as a fluffy dry powder from cotton filter paper (Advantec) via a typical acid hydrolysis protocol⁸ at 50 °C for 3.5 hours followed by, centrifugation, dialysis, sonication and freeze-drying. Polyurethane foam was prepared via in-situ polymerisation. First, PKObP at 61.2 wt.% , catalyst (tin at 0.9 wt.% and amine catalyst at 0.3 wt.%), surfactant Tegostab B8905 at 2 wt.%, and water at 1.5 wt.% (blowing agent) were mixed together in a paper cup and stirred vigorously at 500 rpm for 20 minutes. Subsequently, the pMDI at 34 wt. % was added and mixed for 20 seconds. For the nanocomposite foam, 0.4 wt.% CNC was vigorously mixed and followed by sonication process for 30 minutes in the PKObP. This CNC-PKObP dispersion was then mixed with other chemicals (catalyst, surfactant, and blowing agents) followed with the mixing with pMDI. The mixture (both neat and nanocomposites) were then left to freely rise and cured at room temperature for a week prior to the characterization.

Characterization

The obtained CNC was characterised in terms of morphology, and % crystallinity. The morphology of CNC was studied by transmission electron microscopy in a JEOL 1011 TEM (JEOL, Japan) at 100 kV, and the images were captured by IS Morada 4K CCD camera system. % crystallinity was confirmed using X-ray diffraction (XRD) and Differential Scanning Calorimetry (DSC). XRD was generated at a 40 kV and a current of 40 mA. Samples were scanned at 2°C/min in the range of $2\theta = 1^{\circ}$ - 40° using a step size of 0.02° . Cellulose powders were lightly pressed and flattened to obtain a smooth surface prior to testing. DSC measurements were carried out on a Mettler Toledo DSC 1 Star using aluminium crucible standard 40 μ l. The samples weighed from ~ 6-10 mg and the heating range was between 25 °C and 200°C

ATR-FTIR was also performed on a Thermo-Nicolet 5700 to study the chemical structure of both CNC and PUF. The morphology of foams was studied with an optical microscope (Stereo Microscope, Olympus SZH10) and a Neoscope JCM-5000 (JEOL, Tokyo, Japan) operating at 10 kV. Mechanical testing were performed on an Instron model 5543 universal testing machine fitted with a 500 N load cell. Tensile tests were performed according to ASTM D 638-08 with dimension: thickness = 5 mm, width = 6 mm and gage length = 25 mm and crosshead speed of 5 mm/min. The compressive strength was conducted according to ASTM C 365M-05 with dimension: diameter of 30 mm, thickness of 10 mm and the crosshead speed was 6 mm/min. Five replicates of each material were used for each testing. Thermo-mechanical properties analysis of the foams was performed on cylindrical shape specimen at compression mode on a Dynamic mechanical analyser (DMA) (Simultaneous differential thermal analysis

(SDTA) 861°, Mettler Toledo, GmbH, Switzerland). Specimens were tested at a frequency of 1 Hz over a temperature range between -75 to 150 °C with a heating rate of 2 °C/ min.

RESULTS AND DISCUSSION

Isolation of Cellulose Nanocrystals (CNCs)

The hydrolysis of filter paper (cotton) using sulphuric acid produced and yielded CNC at about 75±3%. Their dimensions were measured from transmission electron microscopic images (Figure 1) using Image J analysis software. It can be seen that obtained CNC are typically rod-like shape with the average width, length and aspect ratio about 14.7 ± 4.9 nm, 167.7 ± 23.2 nm and 11.4, respectively. This value is in agreement with the reported values of cotton CNC obtained via sulfuric acid hydrolysis.⁹⁻¹¹

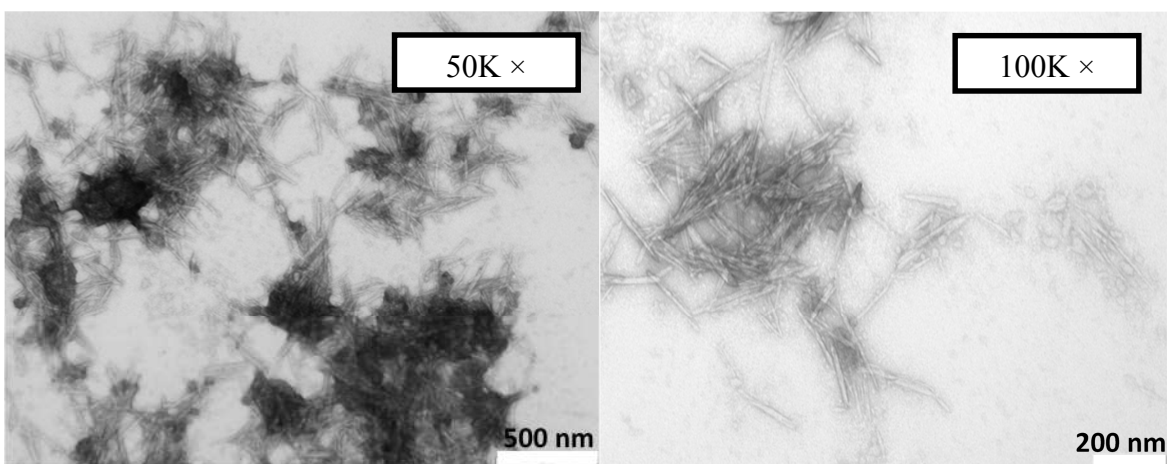


FIGURE 1. TEM images of cellulose nanocrystals obtained via acid hydrolysis. Their dimensions were measured using image J software and averaged from at least 25 measurements

Figure 2 compares FTIR spectra of raw cellulose (filter paper) and obtained CNC via acid hydrolysis. Though the peaks with maximum height at 3332.66 cm^{-1} (for O-H stretching), 1323.95 cm^{-1} (O-H bending) and at 1206 cm^{-1} (C-O stretching) were observed for both samples, CNC exhibited the higher intensity of FTIR spectrum compared to filter paper, which most likely related to the transparency, and higher surface area of cellulose nanocrystals.

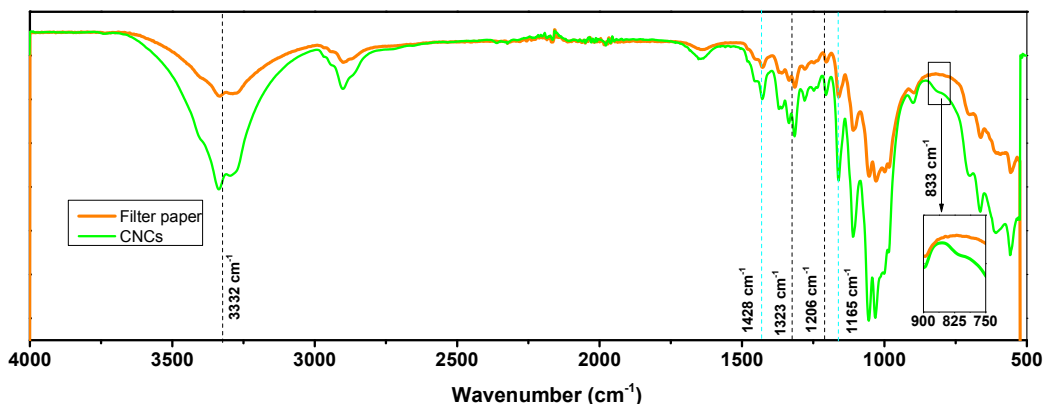


FIGURE 2. FTIR spectra of cellulose before and after hydrolysis

In addition, as can be seen in Figure 3, the chain scission and the removal of amorphous components occurring during acid hydrolysis leads to the formation of sulphate groups on the surface of CNC. The presence of sulphate groups can be observed from peaks at 1165 cm^{-1} and 1428 cm^{-1} corresponds to symmetric S=O (1200 - 1150 cm^{-1}) and

asymmetric ($1430\text{-}1330\text{ cm}^{-1}$) S=O stretching vibrations, respectively. However, these peaks may also merge with glucosic ring vibrations. Despite the fact that the FTIR spectra of CNC is weak in the region indicating S=O, this result is similar to Lu and Hsieh ¹². A weaker and broader peak observed at 833 cm^{-1} may also correspond to the stretching vibration C-O-S bond of C-O-S-SO₃ group on the surface of CNC (Figure 2).

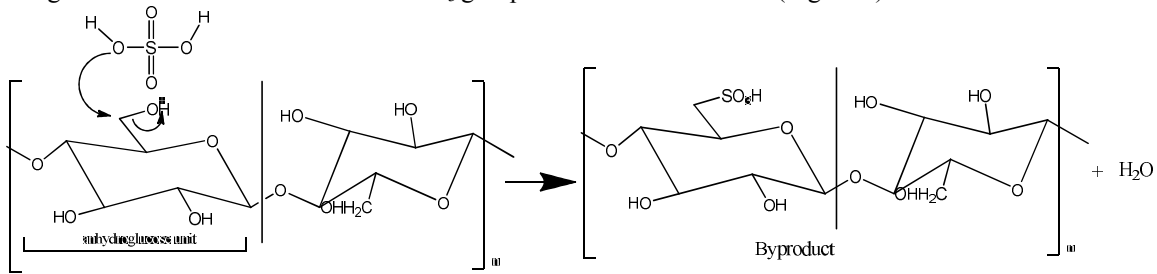


FIGURE 3. Schematic representation of introduction of sulphate groups on the cellulose surface via esterification ¹²

Crystallinity of the cellulose nanocrystals was estimated using X-ray diffractometry (XRD) and differential scanning calorimetry (DSC). Figure 4 shows that the XRD pattern of the CNC was obtained with sharp peaks at 2θ about $22\text{-}23^\circ$, which represented a typical pattern for cellulose II type crystals.

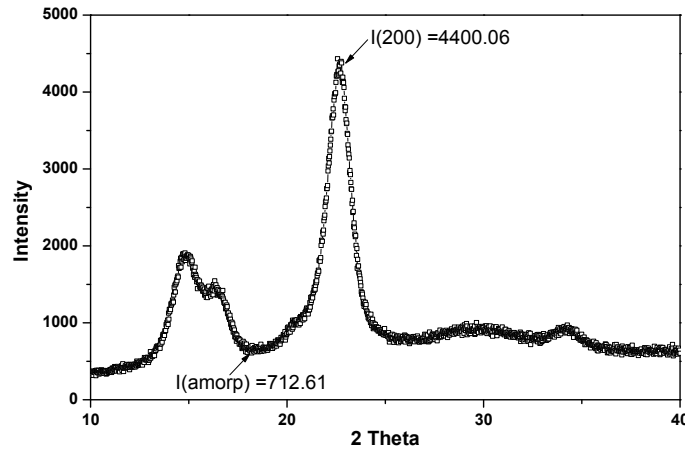


Figure 4. XRD of cellulose nanocrystals

Crystallinity (%) was calculated using Segal's method ¹³ as :

$$\%CC = \frac{I(200) - I(\text{amorphous})}{I200} \times 100\% \quad (1)$$

Where $I_{(200)}$ is the intensity of crystallinity peak at the maximum 2θ between $22^\circ\text{-}23^\circ$, and $I_{(\text{amorphous})}$ is the minimum peak intensity at 2θ between $18^\circ\text{-}19^\circ$ (of amorphous region).

DSC was also performed to confirmed the crystallinity (%) of CNC (Figure 5) using following eq. 2 according to Bertran and Dale ¹⁴.

$$\%CC = \frac{\Delta H_o - \Delta H_s}{\Delta H_o} \times 100\% \quad (2)$$

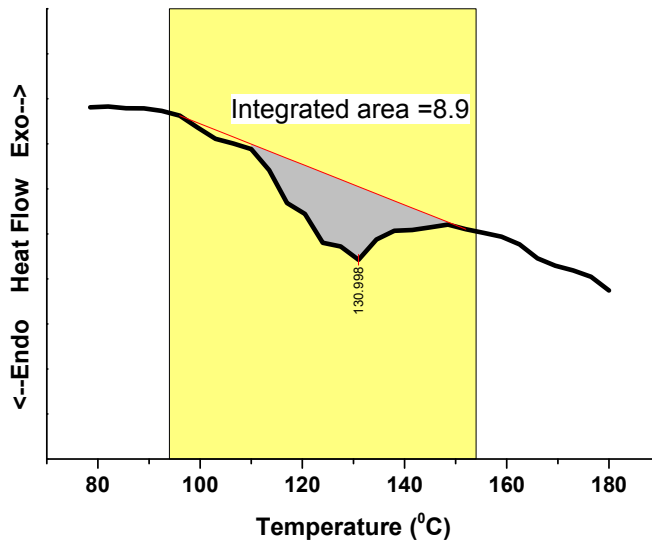


FIGURE 5.DSC of cellulose nanocrystals

In this case, ΔH_0 is the required heat to dehydrate the completely amorphous cellulose, while ΔH_S is the heat required to dehydrate cellulose sample. This equation has also been used by Ciolacu, et al.¹⁵ to measure the crystallinity (%) of CNC. Since, the endothermic dehydration occurs in the same range (110-160 °C) as previously reported study,¹⁴ hence it was considered to use the standard heat of dehydration as $\Delta H_0 = 51.6$ cal/g to calculate the % crystallinity.¹⁴

By using eq. (1) and eq. (2), the % CC by XRD and DSC were 82.8 % and 83.8% respectively which was in a closer agreement with Camarero Espinosa, et al.⁹ where 85 % CC was reported.

Biobased nanocomposite foams reinforced with CNC

Morphological structure of PUF

Figure 6 compares optical micrographs of control neat and nanocomposite foams where bigger and more open cells were observed on both foams. It is expected as this is in agreement with other studies of the reinforcement effect by various nanoscale particles in the PUF matrix, for example, clay,¹⁶ and carbon nanotubes.¹⁷ They reported that nanofiller could act as cell openers and thus increase the open cell number of the foam structure. Further, the bigger cell was observed in the nanocomposite foam. This was due to inhomogeneous cell distribution that might be related to the poor dispersion of CNC as the nanofiller dispersion in this study was prepared by low intensity of ultrasonication process at 50 Hz for 60 minutes. Here, it is suggested to use a higher intensity of ultrasonication process (i.e., 20 KHz) to optimize the dispersion quality for further study.

Further, it was very interesting to note that despite the fact that cell size increased and more open cells were obtained, apparent density of the nanocomposite foam was observed to be higher (68.2 ± 0.8 kg/m³) than that of neat foam (53.8 ± 0.6 kg/m³) which might be related to the broken and thicker cell walls. It is assumed that the inclusion of cellulose nanocrystals might be higher in struts.¹⁸ The higher density might also be related to better mechanical properties and retainment of original shape.¹⁹

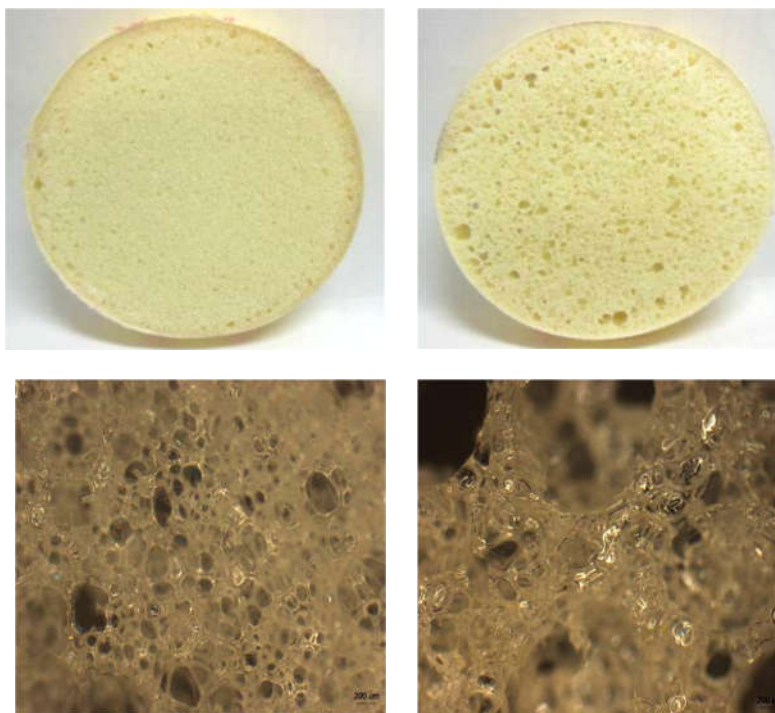


FIGURE 6. Photograph (above) and optical micrographs (below) of the neat (left) and nanocomposite (right) foams (scale bar: 200 μm)

Thermal Properties

In general, degradation of PUF occurs in two steps, at first, the degradation of soft segment associated with degradation of urethane linkage followed by the degradation of hard segment.^{20,21} In Figure 7, we can clearly see that the initial degradation occurs from 205 $^{\circ}\text{C}$, followed by second degradation at around 350 $^{\circ}\text{C}$ for neat PU foam.

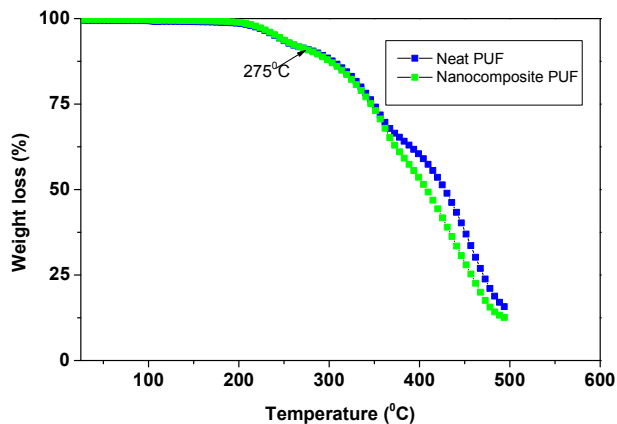


FIGURE 7. Thermograms of neat and nanocomposite (with 0.4 wt. % CNCs) foam

The incorporation of 0.4 wt. % CNC did not significantly affect the initial degradation step (starts around at 205 $^{\circ}\text{C}$), but the degradation starts slightly earlier than that for neat bio-based foam at above 275 $^{\circ}\text{C}$. This might be related to the facilitation of degradation mechanism by sulphate charges on the surface of CNC.

Mechanical Properties

Tensile and compressive of the PUF were measured with at least five specimens according to ASTM D 638-08 and ASTM C 365M-05 respectively.²² It can be seen in Figure 8 that the incorporation of CNC did not significantly improve the tensile strength and strain, which is most likely may be due to the poor dispersion of CNC as a note by the bigger foam cell structure (Figure 6).

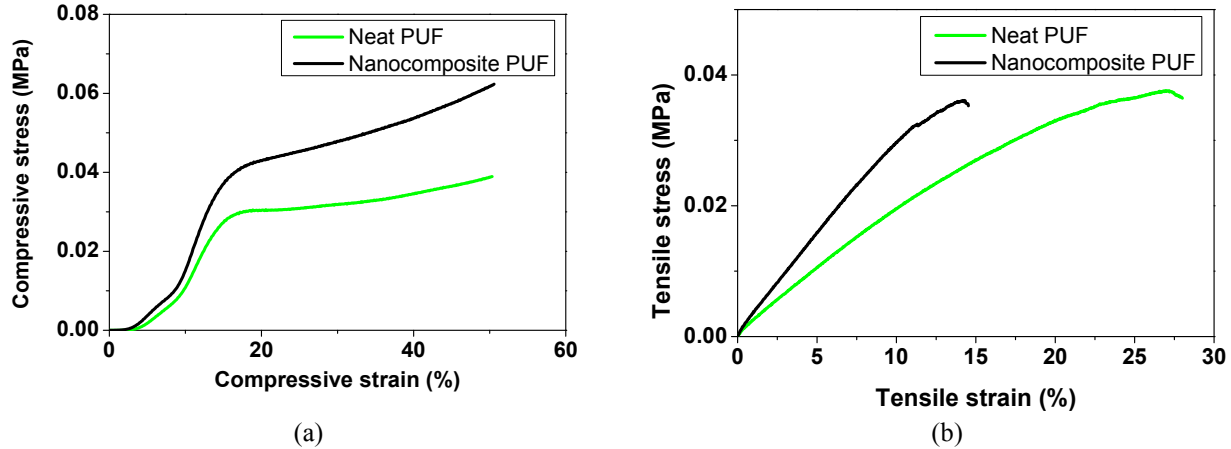


FIGURE 8. Compressive (a) and Tensile (b) and stress-strain of neat PUF and composite PUF

TABLE 1. Compressive and tensile properties of control and nanocomposite biobased PUF

CNCs (Wt.%)	Compressive modulus (kPa)		Compressive strength (kPa)		Tensile strength (kPa)	
	Mean \pm SD	Gain (%)	Mean \pm SD	Gain (%)	Mean \pm SD	Gain (%)
0	560.7 \pm 12.0	--	40.5 \pm 1.3	--	39.3 \pm 5.4	--
0.4	706.6 \pm 29.6	26.0	62.3 \pm 0.8	53.6	39.6 \pm 4.7	0.6

Nevertheless, the compressive strength and modulus dramatically improved by 53.6% and 26.0 % respectively with the presence of 0.4 wt.% CNC (Table 1, Figure 8 (left)). It is expected as generally the incorporating of rigid particles into polymer matrix can simultaneously enhance the stiffness and modulus of composite polymer since they are generally stiffer than polymer.²³ In this case, CNC exhibited excellent mechanical properties especially the axial modulus even greater than Kevlar[®].¹ Hence, when the stress applied during compressive test, the force of pressure can effectively transfer from polymer matrix to nanoparticles and thus provide better ability to support the weight and pressure leading to improved compressive properties.²³

Thermomechanical Properties

Thermo-mechanical properties of PUF were also investigated by dynamic mechanical analyser (DMA) under compression mode. Figure 9 shows the changes in storage modulus and $\tan \delta$ of the biobased foams with and without CNC, in the temperature range from -75 to 150 °C. The storage modulus at room temperature (25 °C) increases almost two fold from 0.7 MPa to 1.3 MPa (~86 %) upon the incorporation of 0.4 wt. % CNC. This significant improvement of storage modulus indicating the aforementioned physical reinforcement effect of rigid nanoparticles of CNC in the PUF matrix.

In terms of thermal transition, it is typical difficult to determine the glassy to rubbery transition of the flexible foams because of their cellular voids and air-trapped area.^{24,25} A $\tan \delta$ curve showing the transition of a foam sample from glassy state to a rubbery state (T_g) denoted as a visible peak displayed in the DMA results. As can be seen in the Figure 9, T_g was found between 60 and 70 °C and there was insignificant change of T_g of PUF with and without

CNC incorporation which is again most likely due to lack interaction between CNC and PUF matrix as a note by the bigger foam cell structure (Figure 6) as well as insignificant improvement of tensile strength (Table 1).

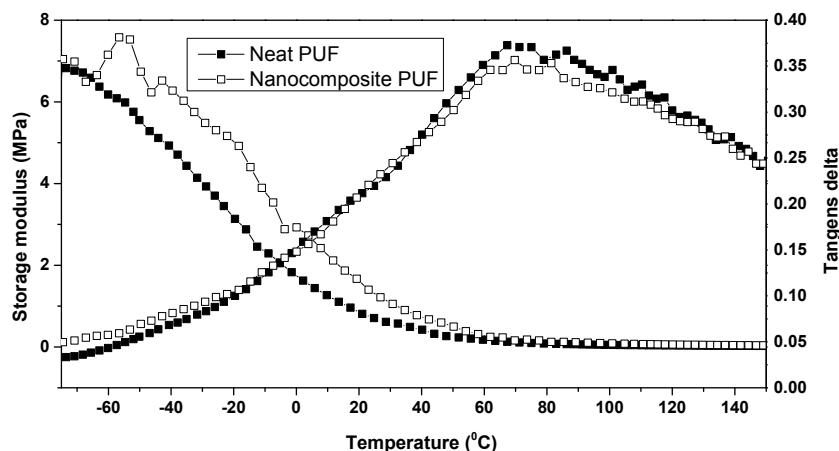


FIGURE 9. Dynamic mechanical properties of neat and nanocomposite biobased PUF

CONCLUSIONS

Rod-like cellulose nanocrystals (CNC) were successfully isolated from cotton resources via acid hydrolysis. The average width, length, aspect ratio and % crystallinity of CNC were found at about 14.7 ± 4.9 nm, 167.7 ± 23.2 nm, 11.4 and, 83 %, respectively. This obtained CNC was then incorporated as reinforcing fillers with the aim to enhance the mechanical properties of final PUF. It was found that the incorporation of low loading CNC at only 0.4 % wt. could dramatically improve the compressive strength and modulus by 53.6% and 26.0 % respectively. The storage modulus at room temperature (25 °C) was also increased almost two fold from 0.7 MPa to 1.3 MPa (~86 %) upon the incorporation of 0.4 wt. % CNC. This significant improvement of storage modulus indicating the aforementioned reinforcement effect of rigid nanoparticles of CNC in the PUF matrix and so the force of pressure can effectively transfer from polymer matrix to nanoparticles and thus provide better ability to support the weight and pressure leading to improve mechanical properties of PUF.

ACKNOWLEDGMENTS

Athanasia Amanda Septevani was gratefully acknowledgement the financial support of Australia Awards Scholarship and funds from INSINAS-RISTEK No. 048/P/RPL-LIPI/INSINAS-2/VI/2017.

REFERENCES

1. Moon, R. J., Martini, A., Nairn, J., Simonsen, J. & Youngblood, J. Cellulose nanomaterials review: structure, properties and nanocomposites. *Chemical Society reviews***40**, 3941-3994, doi:10.1039/c0cs00108b (2011).
2. Eichhorn, S. J., Dufresne, A., Aranguren, M., Marcovich, N. E., Capadona, J. R., Rowan, S. J., Weder, C., Thielemans, W., Roman, M., Renneckar, S., Gindl, W., Veigel, S., Keckes, J., Yano, H., Abe, K., Nogi, M., Nakagaito, A. N., Mangalam, A., Simonsen, J., Benight, A. S., Bismarck, A., Berglund, L. A., Peijs, T..Review: current international research into cellulose nanofibres and nanocomposites. *Journal of Materials Science***45**, 1-33, doi:10.1007/s10853-009-3874-0 (2009).
3. Eichhorn, S. J. Cellulose nanowhiskers: promising materials for advanced applications. *Soft Matter***7**, 303-315, doi:10.1039/c0sm00142b (2011).
4. Habibi, Y., Lucia, L. A. & Rojas, O. J. Cellulose Nanocrystals: Chemistry, Self-Assembly, and Applications. *Chemical Reviews***110**, 3479–3500 (2010).
5. Fong, M. N. F. & Salimon, J. Epoxidation of Palm Kernel Oil Fatty Acids. *Journal of Science and Technology***4**, 87-97 (2013).

6. Badri, K. H. in *Polyurethane* (InTech, 2012).
7. Badri, K. H., Ahmad, S. H. & Zakaria, S. Production of a High-Functionality RBD Palm Kernel Oil-Based Polyester Polyol. *Journal of Applied Polymer Science***81**, 384–389 (2001).
8. Annamalai, P. K., Dagnon, K. L., Monemian, S., Foster, E. J., Rowan, S. J., & Weder, C. Water-responsive mechanically adaptive nanocomposites based on styrene-butadiene rubber and cellulose nanocrystals-processing matters. *ACS applied materials & interfaces***6**, 967-976, doi:10.1021/am404382x (2014).
9. Camarero Espinosa, S., Kuhnt, T., Foster, E. J. & Weder, C. Isolation of thermally stable cellulose nanocrystals by phosphoric acid hydrolysis. *Biomacromolecules*, doi:10.1021/bm400219u (2013).
10. Roohani, M., Habibi, Y., Belgacem, N. M., Ebrahim, G., Karimi, A. N., Dufresne, A. Cellulose whiskers reinforced polyvinyl alcohol copolymers nanocomposites. *European Polymer Journal***44**, 2489-2498, doi:10.1016/j.eurpolymj.2008.05.024 (2008).
11. Capadona, J. R., Van Den Berg, O., Capadona, L. A., Schroeter, M., Rowan, S. J., Tyler, D. J., Weder, C. A versatile approach for the processing of polymer nanocomposites with self-assembled nanofiber templates. Supplementary Information. *Nature nanotechnology* (2007).
12. Lu, P. & Hsieh, Y.-L. Preparation and properties of cellulose nanocrystals: Rods, spheres, and network. *Carbohydrate polymers***82**, 329-336, doi:10.1016/j.carbpol.2010.04.073 (2010).
13. Yu, H., Qin, Z., Liang, B., Liu, N., Zhou, Z., Chen, L. Facile extraction of thermally stable cellulose nanocrystals with a high yield of 93% through hydrochloric acid hydrolysis under hydrothermal conditions. *Journal of Materials Chemistry A*, doi:10.1039/c3ta01150j (2013).
14. Bertran, M. S. & Dale, B. E. Determination of Cellulose Accessibility by Differential Scanning Calorimetry. *Journal of Applied Polymer Science*,**32**, 4241-4253 (1986).
15. Ciolacu, D., Ciolacu, F. & Popa, V. I. Amorphous Cellulose – Structure and Characterization. *Cellulose Chemistry And Technology***45**, 13-21 (2011).
16. Harikrishnan, G., Patro, T. U. & Khakha, D. V. Polyurethane Foam-Clay Nanocomposites: Nanoclays as Cell Openers. *Industrial & Engineering Chemistry Research* **45**, 7126-7134 (2006).
17. Bandarian, M., Shojaei, A. & Rashidi, A. M. Thermal, mechanical and acoustic damping properties of flexible open-cell polyurethane/multi-walled carbon nanotube foams: effect of surface functionality of nanotubes. *Polymer International***60**, 475-482, doi:10.1002/pi.2971 (2011).
18. Pardo-Alonso, S., Solórzano, E., Brabant, L., Vanderniepen, P., Dierick, M., Van Hoorebeke, L., Rodríguez-Pérez, M. A. 3D Analysis of the progressive modification of the cellular architecture in polyurethane nanocomposite foams via X-ray microtomography. *European Polymer Journal***49**, 999-1006, doi:10.1016/j.eurpolymj.2013.01.005 (2013).
19. Polyurethane Foam Association. in *INTOUCH* Vol. 1 (Polyurethane Foam Association, Inc, USA, 1991).
20. Mir Mohammad Alavi Nikje, E. D., and Haghshenas, M. Nanoclay-Flexible Polyurethane Nanocomposites Formulated by Recycled Polyether Polyols. *Cellular Polymers***31**, 257-267 (2012).
21. David, J. *et al.* Development of novel environmental friendly polyurethane foams. *Environmental Chemistry Letters***8**, 381-385, doi:10.1007/s10311-009-0236-8 (2009).
22. Ragauskas, A. J., Li, Y. & Ren, H. Rigid polyurethane foam reinforced with cellulose whiskers: Synthesis and characterization. *Nano-Micro Letters***2**, 89-94, doi:10.5101/nml.v2i2.p89-94 (2010).
23. Fu, S.-Y., Feng, X.-Q., Lauke, B. & Mai, Y.-W. Effects of particle size, particle/matrix interface adhesion and particle loading on mechanical properties of particulate-polymer composites. *Composites Part B: Engineering***39**, 933-961, doi:10.1016/j.compositesb.2008.01.002 (2008).
24. Das, S., Dave, M. & Wilkes, G. L. Characterization of flexible polyurethane foams based on soybean-based polyols. *Journal of Applied Polymer Science***112**, 299-308, doi:10.1002/app.29402 (2009).
25. Gu, R. & Sain, M. M. Effects of Wood Fiber and Microclay on the Performance of Soy Based Polyurethane Foams. *Journal of Polymers and the Environment***21**, 30-38, doi:10.1007/s10924-012-0538-y (2012).